Andreev reflection spectroscopy as a probe for quantum transport through high spin molecules

Subhajit Pal and Colin Benjamin*
School of Physical Sciences, National Institute of Science Education & Research, HBNI, Jatni-752050, India

The ground state properties of a high spin molecule and its interaction with an electronic spin are probed via Andreev reflection. We see that through the charge and spin conductance one can effectively estimate the interaction strength, the ground state spin and magnetic moment of any high spin molecule or for that matter any magnetic impurity. We also show how a high spin molecule at the junction between a normal metal and superconductor can contribute to superconducting spintronics applications. Particularly, while spin conductance is absent below the gap for Ferromagnet-Insulator-Superconductor junctions we show that in the case of a Normal metal-High spin molecule-Normal Metal-Insulator-Superconductor(NMNIS) junction it is present. Further, we show pure spin conduction without any accompanying charge conduction in specific regimes of the NMNIS junction.

arXiv:1612.02796v1 [cond-mat.mes-hall] 8 Dec 2016

I. INTRODUCTION

Andreev reflection, the process of an incident electron(hole) being retro-reflected as a hole(electron) at a interface with a superconductor has been used as a spectroscopic probe for the amount of polarization in ferromagnet's[1,14], to determine the pairing symmetry of High T_c[2,3] and Ferromagnetic superconductors[3] among many other uses. In this work we aim to use it as a spectroscopic tool to completely characterize a high spin molecule, especially its ground state spin, magnetic moment, strength and sign of its interaction with charge carriers in the system. High spin molecules(HSM) or single molecule magnets (SMM) have been around for 20 years or more. The main purpose of research in these is to design molecular magnets however another important direction is towards controlled concoction of stable high spin molecular complexes and their complete characterization, as regards the ground state spin properties of these molecules. For example, how these molecules interact with electron spin, their ground state spin and magnetic moment have been only deciphered via spectroscopic probes like- pulsed electron paramagnetic resonance(EPR)[4], electron nuclear double resonance spectroscopy(ENDOR)[5] or electron spin echo envelope modulation(ESEEM) techniques. The problem with the aforesaid spectroscopic tools like EPR, ENDOR, EESEM, etc are that they only probe one of the features like EPR and ENDOR can only probe the ground state spin while magnetic moment can be done only with EESEM techniques. New techniques like infrared spectroscopy and magnetic circular dichroism spectroscopy have also been invoked recently[6] to fully characterize HSM's, but as already mentioned the multiplicity of spectroscopic techniques increases the complexity of the problem. We propose that Andreev reflection spectroscopy unlike the aforementioned techniques can be a "one stop shop" for characterizing the spin, magnetic moment and the exchange interaction of a HSM thus reducing the complexity involved.

In this work we not only show that Andreev reflection[11] can be an excellent tool to probe these aforesaid aims, we also explore the possibilities of utilizing high spin molecules in superconducting spintronics applications. High spin molecules(HSM) are of great import in molecular spintronics. They belong to the class of mettalo-organic compounds that portray superparamagnetic nature under a particular blocking temperature. These molecules can now be produced, for example, the molecule manganese acetate($Mn_{12} - ac$), which has a large ground state spin ($S = 10$), and a very slow relaxation of magnetization at low temperature. These molecules do not just have integer spin; a number of HSMs exist which have large half-integer spins like the Fe_{19}-complex[12] with a spin of $S = 33/2$. The Hamiltonian[8] for a HSM is given by-

$$H_{HSM} = -DS_z^2 - J_0 \vec{s}.\vec{S} \tag{1}$$

Here first term represents the energy of the HSM. D is an uniaxial anisotropy constant and S_z is the z component of the spin of the HSM. The second term is most relevant in our study as this deals with electron transport. The electrons interact with HSM only via the exchange term $-J_0 \vec{s}.\vec{S}$, with J_0 being the strength of the exchange interaction, $\vec{s}$ is the electronic spin and $\vec{S}$ is the spin of the HSM or magnetic impurity. Furthermore, the magnitude of D in a realistic HSM is very small compared to J_0[9]. The first term is only relevant in electronic structure calculations but it's not relevant for electronic transport calculations. Thus, the only term of interest in our aims to use Andreev reflection as a spectroscopic probe to characterize a HSM and for spintronics applications is the exchange coupling(2nd term). The exact setting we will use is shown in Fig. 1, it shows a HSM at $x = 0$ and a delta potential barrier at $x = a$. In the regions I($x < 0$) and II($0 < x < a$) there are two normal metals while for $x > a$ there is a s-wave superconductor. We study the Andreev reflection enabled transport across this junction especially concentrating on

below the gap regime of the superconductor. We consider unpolarized electrons incident at the junction and show how the differential charge and spin conductance vary with the impurity spin S and z-component of the impurity spin m' respectively. From the values of the differential spin and charge conductance we can get the exact values of the exchange interaction strength, ground state spin and magnetic moment of the molecule. We also study the spin and charge conductance through the junction and its possible applications in superconducting spintronics[7]. Particularly, we focus on conditions for obtaining pure spin conductance in absence of any charge conductance. Thus the twin objectives of this study are: A. To characterize the ground state spin, magnetic moment and exchange interaction of a HSM and B. To exploit quantum transport across this Normal Metal-HSM-Normal Metal-Insulator-Superconductor(NMNIS) junction to design a pure spin conducting device. The rest of the paper are organized as follows: in the succeeding section (Theory), we first outline a brief sketch of our set-up and provide a theoretical background to our study by writing the Hamiltonian and solving the equations after imposing boundary conditions on the wavefunctions. We plot the Andreev and normal reflection probabilities and see the effect of the spin of HSM on these probabilities both for transparent as well as tunneling regimes. We also define the differential charge and spin conductance and give expressions for both the conductances in certain limits. We end the "Theory" section by tabulating all the results for the charge and spin conductance in a table. The section after Theory deals with the first objective of this work, i.e. characterization, in three separate subsections as well as two extensive tables and three elaborate figures we explain the way to characterize the HSM via only the differential charge and spin conductance. The section after characterization deals with the second aim of this work namely applications in superconducting spintronics, we show how we can utilize our set-up to have pure spin conductance in absence of any charge conductance. Finally we conclude our study with a section on conclusion and a perspective on future endeavors. We also provide an Appendix wherein details of the calculations are provided.

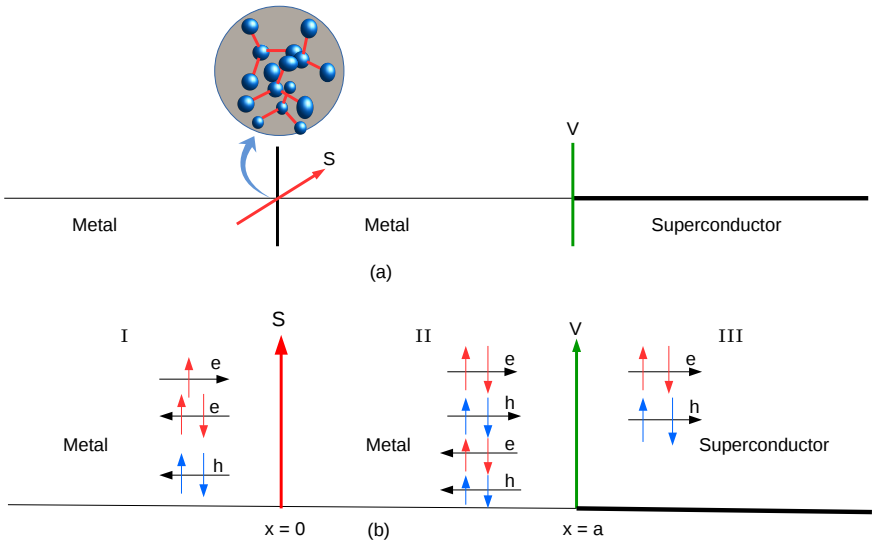

FIG. 1: (a) A high spin molecule with spin S and magnetic moment m' at $x = 0$ in a Normal Metal-HSM-Normal Metal-Insulator-Superconductor(NMNIS) junction, (b) The scattering of an up-spin electron incident is shown. Andreev reflection and quasi particle transmission into superconductor are depicted. For details see section II B.

II. THEORY

A. Hamiltonian

We consider a metal(N)-metal(N)-superconductor(S) junction where there is a HSM between two metallic regions at $(x = 0)$ and a δ-like potential barrier exists at metal superconductor interface at $(x = a)$. When an electron with energy E and spin($\uparrow$ / $\downarrow$) is incident from the normal metal, at the $x = 0$ interface it interacts with the HSM through an exchange potential which may induce a mutual spin flip. The electron can be reflected back to region I,

or transmitted to region II, with spin up or down. When this transmitted electron is incident at $x = a$ interface it could be reflected back from the interface and there is also possibility of Andreev reflection, i.e., a hole with spin up or down is reflected back to region II. Electron-like and hole-like quasiparticles with spin up or down are transmitted into the superconductor for energies above the gap.

The model Hamiltonian in Bogoliubov-de Gennes formalism of our Normal Metal-Insulator-Magnetic Molecule-Normal Metal-Superconductor system is given below:

$$\begin{bmatrix} H & \Delta\theta(x-a) \\ \Delta^*\theta(x-a) & -H \end{bmatrix} \Psi(x) = E\Psi(x), \text{ with } H = p^2/2m^\star + V\delta(x-a) - J_0\delta(x)\vec{s}.\vec{S} - E_F,$$

Ψ is a four-component spinor, Δ is the gap in s-wave superconductor and θ is the Heaviside s

Further in H the first term is the kinetic energy of an electron with effective mass $m^\star$, for second term V is the strength of the δ-like potential at the interface between normal metal and superconductor and the third term describes the exchange interaction of strength J_0 between the electron with spin $\vec{s}$ and a magnetic molecule with spin $\vec{S}$, E_F being the Fermi energy.

B. Wavefunctions

The Wavefunctions of the different region of the system as shown in FIG. 1(a) and FIG. 1(b) can be written in spinorial form[10]:

$$\psi_N^I(x) = \begin{bmatrix}1\\0\\0\\0\end{bmatrix} e^{ik_e x}\phi^S_{m'} + r_e^{\uparrow\uparrow}\begin{bmatrix}1\\0\\0\\0\end{bmatrix} e^{-ik_e x}\phi^S_{m'} + r_e^{\uparrow\downarrow}\begin{bmatrix}0\\1\\0\\0\end{bmatrix} e^{-ik_e x}\phi^S_{m'+1} + r_h^{\uparrow\uparrow}\begin{bmatrix}0\\0\\1\\0\end{bmatrix} e^{ik_h x}\phi^S_{m'} + r_h^{\uparrow\downarrow}\begin{bmatrix}0\\0\\0\\1\end{bmatrix} e^{ik_h x}\phi^S_{m'+1}, \text{for } x<0$$

$$\Psi_N^{II}(x) = t_e^{'\uparrow\uparrow}\begin{bmatrix}1\\0\\0\\0\end{bmatrix} e^{ik_e x}\phi^S_{m'} + t_e^{'\uparrow\downarrow}\begin{bmatrix}0\\1\\0\\0\end{bmatrix} e^{ik_e x}\phi^S_{m'+1} + b_e^{\uparrow\uparrow}\begin{bmatrix}1\\0\\0\\0\end{bmatrix} e^{-ik_e(x-a)}\phi^S_{m'} + b_e^{\uparrow\downarrow}\begin{bmatrix}0\\1\\0\\0\end{bmatrix} e^{-ik_e(x-a)}\phi^S_{m'+1}$$

$$+c_h^{\uparrow\uparrow}\begin{bmatrix}0\\0\\1\\0\end{bmatrix} e^{ik_h(x-a)}\phi^S_{m'} + c_h^{\uparrow\downarrow}\begin{bmatrix}0\\0\\0\\1\end{bmatrix} e^{ik_h(x-a)}\phi^S_{m'+1} + a_h^{\uparrow\uparrow}\begin{bmatrix}0\\1\\0\\0\end{bmatrix} e^{-ik_h x}\phi^S_{m'} + a_h^{\uparrow\downarrow}\begin{bmatrix}0\\0\\0\\1\end{bmatrix} e^{-ik_h x}\phi^S_{m'+1}, \text{for } 0<x<a$$

$$\psi_S(x) = t_e^{\uparrow\uparrow}\begin{bmatrix}u\\0\\0\\v\end{bmatrix} e^{iq_+ x}\phi^S_{m'} + t_e^{\uparrow\downarrow}\begin{bmatrix}0\\u\\v\\0\end{bmatrix} e^{iq_+ x}\phi^S_{m'+1} + t_h^{\uparrow\uparrow}\begin{bmatrix}0\\v\\u\\0\end{bmatrix} e^{-iq_- x}\phi^S_{m'} + t_h^{\uparrow\downarrow}\begin{bmatrix}v\\0\\0\\u\end{bmatrix} e^{-iq_- x}\phi^S_{m'+1}, \text{for } x>a$$

$r_e^{\uparrow\uparrow}(r_e^{\uparrow\downarrow})$ and $r_h^{\uparrow\uparrow}(r_h^{\uparrow\downarrow})$ are the corresponding amplitudes for normal reflection and Andreev reflection with spin up(down). $t_e^{\uparrow\uparrow}(t_e^{\uparrow\downarrow})$ and $t_h^{\uparrow\uparrow}(t_h^{\uparrow\downarrow})$ are the corresponding amplitudes for transmission of electron-like quasiparticles and hole-like quasiparticles with spin up(down). $\phi^S_{m'}$ is the eigenfunction of magnetic impurity: with its S^z operator acting as- $S^z\phi^S_{m'} = m'\phi^S_{m'}$, with m' being the spin magnetic moment of the HSM. For $E > \Delta$(for energies above the gap),the coherence factors are $u^2 = \frac{1}{2}\left[1 + \frac{(E^2-\Delta^2)^{\frac{1}{2}}}{E}\right]$, $v^2 = \frac{1}{2}\left[1 - \frac{(E^2-\Delta^2)^{\frac{1}{2}}}{E}\right]$, while the wave-vector in metal is $k_{e,h} = \sqrt{2m^\star(E_F \pm E)}$ and in superconductor is $q_\pm = \sqrt{2m^\star(E_F \pm \sqrt{E^2-\Delta^2})}$ and for $E < \Delta$(for energies below the gap) the coherence factors are $u^2 = \frac{1}{2}\left[1 + i\frac{(\Delta^2-E^2)^{\frac{1}{2}}}{E}\right]$, $v^2 = \frac{1}{2}\left[1 - i\frac{(\Delta^2-E^2)^{\frac{1}{2}}}{E}\right]$, while the wavevector in metal is $k_{e,h} = \sqrt{2m^\star(E_F \pm E)}$ and in superconductor is $q_\pm = \sqrt{2m^\star(E_F \pm i\sqrt{\Delta^2-E^2})}$[11], with E_F the Fermi energy, m^* being effective mass of electron in metal and E is the excitation energy of electron above E_F. In Andreev approximation, which we will use throughout this work, $E_F \gg \Delta, E$ we take $k_e = k_h = q_+ = q_- = k_F$ We impose the boundary conditions on the above wave-functions and solve the resulting 16 equations and get the different scattering amplitudes: $r_e^{\uparrow\uparrow}, r_e^{\uparrow\downarrow}, r_h^{\uparrow\uparrow}, r_h^{\uparrow\downarrow}, t_e^{\uparrow\uparrow}, t_e^{\uparrow\downarrow}, t_h^{\uparrow\uparrow}, t_h^{\uparrow\downarrow}$, see Appendix. The reflection and transmission probabilities we get are thus- $R_{ee}^{\uparrow\uparrow} = |r_{ee}^{\uparrow\uparrow}|^2, R_{ee}^{\uparrow\downarrow} = |r_{ee}^{\uparrow\downarrow}|^2, R_{eh}^{\uparrow\uparrow} = |r_{eh}^{\uparrow\uparrow}|^2, R_{eh}^{\uparrow\downarrow} = |r_{eh}^{\uparrow\downarrow}|^2$, $T_{ee}^{\uparrow\uparrow} = |t_{ee}^{\uparrow\uparrow}|^2, T_{ee}^{\uparrow\downarrow} = |t_{ee}^{\uparrow\downarrow}|^2, T_{eh}^{\uparrow\uparrow} = |t_{eh}^{\uparrow\uparrow}|^2, T_{eh}^{\uparrow\downarrow} = |t_{eh}^{\uparrow\downarrow}|^2$, these are plotted in Figures below.

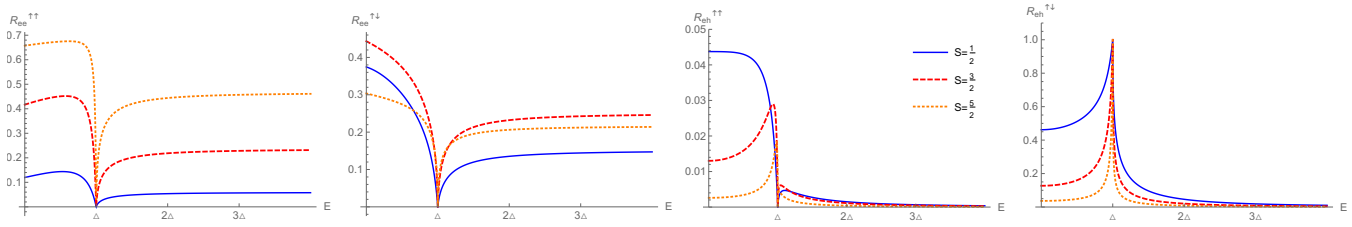

(a) (b) (c) (d)

FIG. 2: a) $J = 1.0, Z = 0.0, m' = -1/2$ *b)* $J = 1.0, Z = 0.0, m' = -1/2$ *c)* $J = 1.0, Z = 0.0, m' = -1/2$ *d)* $J = 1.0, Z = 0.0, m' = -1/2$

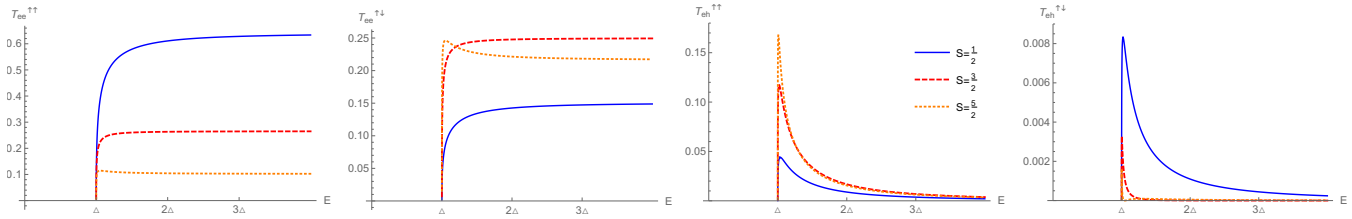

(a) (b) (c) (d)

FIG. 3: a) $J = 1.0, Z = 0.0, m' = -1/2$ *b)* $J = 1.0, Z = 0.0, m' = -1/2$ *c)* $J = 1.0, Z = 0.0, m' = -1/2$ *d)* $J = 1.0, Z = 0.0, m' = -1/2$

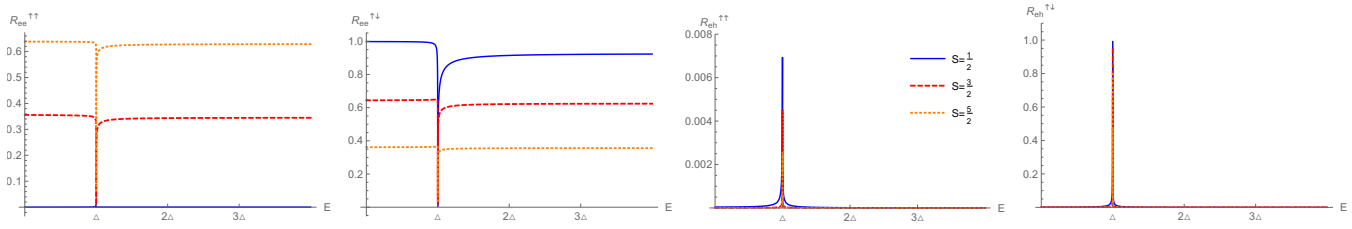

(a) (b) (c) (d)

FIG. 4: a) $J = 1.0, Z = 3.0, m' = -1/2$ *b)* $J = 1.0, Z = 3.0, m' = -1/2$ *c)* $J = 1.0, Z = 3.0, m' = -1/2$ *d)* $J = 1.0, Z = 3.0, m' = -1/2$

C. Andreev Reflection in presence of a HSM

In Fig. 2 we plot the normal and Andreev reflection probabilities with spin-flip or no-flip for different values of the spin of magnetic molecule $S(1/2, 3/2, 5/2)$, we fix the magnetic moment of the molecule- $m' = -1/2$ and we take $Z = 0$- the transparent regime. In Fig. 2(a) we see normal reflection probability without spin flip increases with increase of spin of magnetic molecule (S), while in 2(b) normal reflection probability with spin flip shows a mixed behavior it first increases then decreases with increase of S, this is for the entire range of electron excitation energy. Next in Fig. 2(c) we plot Andreev reflection without spin flip, for increasing spin it continuously decreases for both above as well as below the gap. Finally, in Fig. 2(d) we plot the Andreev reflection probability with spin flip, we find both above as well as below the gap, probability decreases as we spin increase. Thus, for a high spin molecule, normal reflection probability is large but Andreev reflection probability is small. Andreev reflection, hence is inhibited by the spin of magnetic molecule. This behavior, especially for large S, has similarities as well as differences with seen for a Ferromagnet-insulator-Superconductor junction[14]. So, although it is one of the main aims of high spin molecule research to design single molecule magnets, one of the conclusions of our work is that high spin molecules are not Ferromagnets.

In Fig. 3, we plot the quasiparticle transmission probabilities for spin flip and without spin flip for same parameter values as in Fig. 2. Since there is no quasiparticle transmission below the gap we will only focus on above the gap regime. In Fig. 3(a) we show that with increase in spin of magnetic molecule (S) the electron-like quasiparticle transmission without flip decreases on the other hand in Fig. 3(b) with increase in spin of magnetic molecule (S) the electron-like quasiparticle transmission with flip increases. Thus high spin molecules inhibit no flip transmission

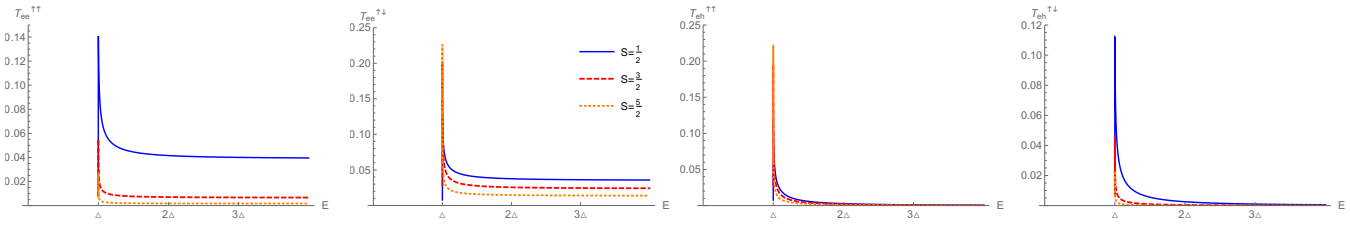

(a) (b) (c) (d)

FIG. 5: a) $J = 1.0, Z = 3.0, m' = -1/2$ *b)*$J = 1.0, Z = 3.0, m' = -1/2$ *c)*$J = 1.0, Z = 3.0, m' = -1/2$ *d)*$J = 1.0, Z = 3.0, m' = -1/2$

but boost transmission with spin-flip for electron-like quasiparticle. In Fig. 3(c) and (d) we plot the probability for hole-like quasiparticle transmission, in (c) we see that with increase in spin of magnetic molecule (S) the probability for no-flip transmission increases while in (d) we see the opposite. Thus high spin molecules show opposite behavior for holes, they inhibit spin-flip transmission while giving a boost to no-flip transmission.

While Figs. 2 and 3 dealt with reflection and transmission in the transparent (Z=0) regime, in Figs. 4 and 5 we deal with the tunneling (Z=3) regime, other parameters remain same. In Fig. 4(a) we see the normal reflection probability in absence of spin flip increases with increase of the spin(S) of magnetic molecule, while the normal reflection probability with spin flip decreases with spin(S). Since in the tunneling regime Andreev reflection by default is inhibited the addition of magnetic molecule enhances normal reflection and further inhibits Andreev reflection for both spin-flip and no-flip cases. Finally, in Fig. 5 we plot the quasiparticle transmission probabilities. We see in all cases increasing spin (S) of magnetic molecule leads to a continuous decrease of both electron-like and hole-like transmission probabilities. Further, in the tunneling regime the differences between spin states of the HSM are almost obliterated.

Similar to above, if we consider an electron with spin down incident from normal metal region I, and get the different reflection and transmission probabilities as follows: $R_{ee}^{\downarrow\uparrow}, R_{ee}^{\downarrow\downarrow}, R_{eh}^{\downarrow\uparrow}, R_{eh}^{\downarrow\downarrow}$, and for quasiparticle transmission above the gap $T_{ee}^{\downarrow\uparrow}, T_{ee}^{\downarrow\downarrow}, T_{eh}^{\downarrow\uparrow}, T_{eh}^{\downarrow\downarrow}$. As we solve for the scattering amplitudes when electron with spin up is incident, we can also do the same for a spin down incident electron. We do not repeat them here but in analogy to spin up case the wavefunctions can be easily written.

D. Charge and Spin conductance

To calculate the total differential spin conductance, we follow the well established definitions as in Ref. [15 and 16]. The spin conductance of the set-up as envisaged in Fig. 1 is given by-

$$G_S^0 = G_S^{\uparrow} - G_S^{\downarrow}$$

where

$$G_S^{\uparrow} = 1 + R_{eh}^{\uparrow\uparrow} - R_{eh}^{\uparrow\downarrow} - R_{ee}^{\uparrow\uparrow} + R_{ee}^{\uparrow\downarrow}$$

and

$$G_S^{\downarrow} = 1 + R_{eh}^{\downarrow\downarrow} - R_{eh}^{\downarrow\uparrow} - R_{ee}^{\downarrow\downarrow} + R_{ee}^{\downarrow\uparrow}$$

So,

$$G_S^0 = R_{eh}^{\uparrow\uparrow} - R_{eh}^{\uparrow\downarrow} - R_{ee}^{\uparrow\uparrow} + R_{ee}^{\uparrow\downarrow} - R_{eh}^{\downarrow\downarrow} + R_{eh}^{\downarrow\uparrow} + R_{ee}^{\downarrow\downarrow} - R_{ee}^{\downarrow\uparrow} \tag{3}$$

while the net differential charge conductance is deined as[15,16]-

$$G_C^0 = G_C^{\uparrow} + G_C^{\downarrow}$$

where

$$G_C^{\uparrow} = 1 + R_{eh}^{\uparrow\uparrow} + R_{eh}^{\uparrow\downarrow} - R_{ee}^{\uparrow\uparrow} - R_{ee}^{\uparrow\downarrow}$$

and

$$G_C^{\downarrow} = 1 + R_{eh}^{\downarrow\uparrow} + R_{eh}^{\downarrow\downarrow} - R_{ee}^{\downarrow\uparrow} - R_{ee}^{\downarrow\downarrow}$$

So,

$$G_C^0 = 2 + R_{eh}^{\uparrow\uparrow} + R_{eh}^{\uparrow\downarrow} - R_{ee}^{\uparrow\uparrow} - R_{ee}^{\uparrow\downarrow} + R_{eh}^{\downarrow\downarrow} + R_{eh}^{\downarrow\uparrow} - R_{ee}^{\downarrow\downarrow} - R_{ee}^{\downarrow\uparrow} \tag{4}$$

where $R_{eh}^{\uparrow\uparrow}$ is the probability of Andreev reflection of an electron(spin up)as hole(spin up).
$R_{eh}^{\uparrow\downarrow}$ is the probability of Andreev reflection of an electron(spin up)as hole(spin down).
$R_{ee}^{\uparrow\uparrow}$ is the probability of normal reflection of an electron(spin up)as electron(spin up).
$R_{ee}^{\uparrow\downarrow}$ is the probability of normal reflection of an electron(spin up)as electron(spin down).
$R_{eh}^{\downarrow\downarrow}$ is the probability of Andreev reflection of an electron(spin down)as hole(spin down).
$R_{eh}^{\downarrow\uparrow}$ is the probability of Andreev reflection of an electron(spin down)as hole(spin up).
$R_{ee}^{\downarrow\downarrow}$ is the probability of normal reflection of an electron(spin down)as electron(spin down).
$R_{ee}^{\downarrow\uparrow}$ is the probability of normal reflection of an electron(spin down)as electron(spin up).

Now for below the gap($-\Delta < E < \Delta$) regime and with spin up electron incident, the conservation of probability gives:

$$R_{eh}^{\uparrow\uparrow} + R_{eh}^{\uparrow\downarrow} + R_{ee}^{\uparrow\uparrow} + R_{ee}^{\uparrow\downarrow} = 1$$

and for spin down electron incident, the conservation of probability gives:

$$R_{eh}^{\downarrow\uparrow} + R_{eh}^{\downarrow\downarrow} + R_{ee}^{\downarrow\uparrow} + R_{ee}^{\downarrow\downarrow} = 1$$

Putting these two conditions in the diferential conductances we get, for below the gap ($-\Delta < E < \Delta$):

$$G_S = \frac{1}{2\pi}\int_0^{2\pi} 2(R_{eh}^{\uparrow\uparrow} + R_{ee}^{\uparrow\downarrow} - R_{eh}^{\downarrow\downarrow} - R_{ee}^{\downarrow\uparrow})d(k_F a) = \frac{1}{2\pi}\int_0^{2\pi} G_S^0 d(k_F a) \tag{5}$$

and

$$G_C = \frac{1}{2\pi}\int_0^{2\pi} 2(R_{eh}^{\uparrow\uparrow} + R_{eh}^{\uparrow\downarrow} + R_{eh}^{\downarrow\downarrow} + R_{eh}^{\downarrow\uparrow})d(k_F a) = \frac{1}{2\pi}\int_0^{2\pi} G_C^0 d(k_F a) \tag{6}$$

1. Differential charge and spin conductance in the transparent (Z=0) regime

After deriving the amplitudes of normal and Andreev reflection by solving the scattering problem, see Appendix, we get an expression for the differential charge and spin conductance in the transparent regime ($Z = 0$) as follows, first the differential spin conductance:

$$G_S^0 = \frac{P_1}{Q_1} - \frac{P_2}{Q_2} \tag{7}$$

where

$$\begin{aligned}
P_1 &= 8J^2(4F_2^2J^2(1+m')^2\Delta^2(\Delta^2-E^2) + F_2^2(\Delta^2-E^2)((-JE+2\sqrt{\Delta^2-E^2} + J^2(F_2^2+m'+m'^2)\sqrt{\Delta^2-E^2})^2 \\
&\quad + (2E + J\sqrt{\Delta^2-E^2})^2)) \\
Q_1 &= 4(4 + J^2(1+2F_2^2+2m'+2m'^2))^2E^2(\Delta^2-E^2) + ((8 + J^4(F_2^2+m'+m'^2)^2 + J^2(2+4F_2^2+4m'+4m'^2))E^2 \\
&\quad - (4 + (1+4F_2^2)J^2 + J^4(F_2^2+m'+m'^2)^2)\Delta^2)^2 \\
P_2 &= 8J^2(4F_4^2J^2(1-m')^2\Delta^2(\Delta^2-E^2) + F_4^2(\Delta^2-E^2)((-JE+2\sqrt{\Delta^2-E^2} + J^2(F_4^2-m'+m'^2)\sqrt{\Delta^2-E^2})^2 \\
&\quad + (2E + J\sqrt{\Delta^2-E^2})^2)) \\
Q_2 &= 4(4 + J^2(1+2F_4^2-2m'+2m'^2))^2E^2(\Delta^2-E^2) + ((8 + J^4(F_4^2-m'+m'^2)^2 + J^2(2+4F_4^2-4m'+4m'^2))E^2 \\
&\quad - (4 + (1+4F_4^2)J^2 + J^4(F_4^2-m'+m'^2)^2)\Delta^2)^2
\end{aligned}$$

The above differential spin conductance expression shows that it is independent of the length in between HSM and Superconductor a, however it is dependent on Δ, electron energy E, exchange interaction magnitude J and its sign and finally it depends on the spin S and magnetic moment m' of the HSM.
Next the differential charge conductance:

$$G_C^0 = \frac{R_1}{Q_1} + \frac{R_2}{Q_2} \tag{8}$$

where

$$\begin{aligned} R_1 = {} & 8\Delta^2(4F_2^2J^4(1+m')^2(\Delta^2-E^2) + (J(1+2m')\sqrt{\Delta^2-E^2}-2E)^2 + (J(E+2m'E)+2\sqrt{\Delta^2-E^2} \\ & + J^2(F_2^2-m'-m'^2)\sqrt{\Delta^2-E^2})^2) \\ R_2 = {} & 8\Delta^2(4F_4^2J^4(1-m')^2(\Delta^2-E^2) + (J(1-2m')\sqrt{\Delta^2-E^2}-2E)^2 + (J(E-2m'E)+2\sqrt{\Delta^2-E^2} \\ & + J^2(F_4^2+m'-m'^2)\sqrt{\Delta^2-E^2})^2) \end{aligned}$$

Similar to the differential spin conductance, the charge expression is also independent of $'a'$, and dependent on Δ, electron energy E, exchange interaction magnitude J and its sign and finally it depends on the spin S and magnetic moment m' of the HSM. The reason this dependence/independence becomes crucial is that these factors become the key determinant for both characterization of HSM as well as in the spintronic applications which will be dealt with in the latter sections.

In the above equations, the spin-flip probabilities for electron is $F_1 = \sqrt{(s+m)(s-m+1)}$ while for magnetic molecule is $F_2 = \sqrt{(S-m')(S+m'+1)}$ for the case when spin-up electron is incident[8,13], while $F_3 = \sqrt{(s-m)(s+m+1)}$ and $F_4 = \sqrt{(S+m')(S-m'+1)}$ are the spin-flip probabilities for electron and high spin molecule when a spin-down electron is incident.

2. Differential charge and spin conductance: The general case

The general formulas for spin and charge conductances are too long to reproduce here, so we especially concentrate on the two limits:
1. the zero bias case $E = 0$, and 2. the gap edge limit $E = \Delta$,
In the first case the expressions become too long to simplify so we further take (a) the $Z = 0$ transparent contact and (b) the $Z = Large$ (tunneling) case.

1(a) The differential charge conductance at zero bias ($E = 0$) for transparent junction ($Z = 0$):

$$G_C^0 = \frac{P}{Q}$$

Where

$$P = 8(128 + 96J^2 + 192F_4^2J^2 + 112F_4^4J^4 + 2J^6 + 32F_4^6J^6 + 4F_4^8J^8 + F_4^8J^{10} + 48J^6m'^2 + 48J^6m'^4 + 6J^{10}m'^4 + 4J^{10}m'^6 + 6J^{10}m'^8 + 24J^4(1+2m'^2)^2 + 8F_4^6J^8(1-2m'+2m'^2) + 32F_4^2J^4(5-5m'+3m'^2) + 8F_4^4J^6(5-8m'+8m'^2) + 4F_4^6J^{10}m'(-1+3m'+4m'^2+2m'^3) + 2F_4^4J^{10}m'^2(5-10m'-3m'^2+8m'^3+8m'^4) + 4F_4^2J^6(11-20m'+36m'^2 + 16m'^3+24m'^4) + F_4^4J^8(3-16m'+72m'^2+16m'^3+56m'^4) + 4F_4^2J^{10}m'^2(2-m'+2m'^2+m'^3+5m'^4+4m'^5+3m'^6) + 2J^8m'^2(3+15m'^2+8m'^4+12m'^6) + 2F_4^2J^8(2-5m'+31m'^2+4m'^4-24m'^5+24m'^6) + J^{12}m'^2(1+m')^2(F_4^8 + 4F_4^6(-1+m')m' + 2(-1+m')^2m'^4(1+m'^2) + F_4^4m'^2(7-10m'+7m'^2) + 2F_4^2m'^2(2-m'+3m'^2-7m'^3+3m'^4))+ F_2^8J^8(4+(1+4F_4^2)J^2 + J^4(F_4^4+(-1+m')^2m'^2+2F_4^2(2-3m'+m'^2))) + 4F_2^6J^6(2+J^2m'(1+m'))(4+(1+4F_4^2)J^2+ J^4(F_4^4+(-1+m')^2m'^2+2F_4^2(2-3m'+m'^2))) + F_2^4J^4(112+8J^2(5+16F_4^2+8m'+8m'^2) + J^4(3+48F_4^4+16m' + 72m'^2-16m'^3+56m'^4+16F_4^2(7-6m'+8m'^2)) + J^8(F_4^8+4F_4^6(-1+m')m'+(-1+m')^2m'^4(7+10m'+7m'^2) + 12F_4^4(m'^2+m'^4)+8F_4^2m'^2(3+m'-3m'^2-3m'^3+2m'^4)) + 2J^6(4F_4^6+2F_4^4(1+8m'^2)+m'^2(5+10m'-3m'^2-8m'^3 + 8m'^4)+4F_4^2(1+6m'+m'^2-4m'^3+8m'^4))) + 2F_2J^2(96+16J^2(5+8F_4^2+5m'+3m'^2)+2J^4(11+32F_4^4+20m' + 36m'^2-16m'^3+24m'^4+16F_4^2(5+4m'^2)) + J^{10}(1+m')(F_4^8(2+m')+4F_4^6m'(-2+m'+m'^2)+8F_4^2m'^4(3-3m' - m'^2+m'^3)+4F_4^4m'^2(3-4m'+m'^2+2m'^3)+(-1+m')^2m'^4(2-m'+4m'^2+3m'^3)) + J^6(2+16F_4^6+5m'+31m'^2 + 4m'^4+24m'^5+24m'^6+8F_4^4(7+6m'+8m'^2)+32F_4^2(1+m'^2+2m'^4)) + 2J^8(F_4^8+8F_4^6(1+m'+m'^2)+4F_4^2m'^2 (3+m'^2+4m'^4)+2F_4^4(1-6m'+m'^2+4m'^3+8m'^4)+m'^2(2+m'+2m'^2-m'^3+5m'^4-4m'^5+3m'^6))))$$

$$Q = (4+(1+4F_4^2)J^2+J^4(F_4^2+(-1+m')m')^2)^2(4+(1+4F_2^2)J^2+J^4(F_2^2+m'+m'^2)^2)^2$$

Looking at the above expression, we can see that the expression is independent of $'a'$ and sign of exchange interaction but dependent on the magnitude of exchange interaction, spin and magnetic moment of HSM.

Similarly, the differential spin conductance at zero bias ($E = 0$ or without any voltage bias applied to normal metal region I) for transparent junction ($Z = 0$):

$$G_S^0 = \frac{R}{Q}$$

Where

$$R = -8J^2(F_2^8F_4^2J^8(4+J^4(F_4^2+(-1+m')m')^2+J^2(5+4F_4^2-12m'+8m'^2))+F_4^2(4+J^2+J^4m'^2(1+m')^2)^2 (4+J^4(F_4^2+(-1+m')m')^2+J^2(5+4F_4^2-12m'+8m'^2))-F_2^6J^4(16+8J^2+J^8(F_4^2+(-1+m')m')^2(F_4^4+ (-1+m')^2m'^2-2F_4^2m'(3+m'))+J^4(1-8F_4^4+8m'^2-16m'^3+8m'^4-32F_4^2(1-2m'+2m'^2))-2J^6(-(-1+m')^2m'^2 + F_4^4(-1+8m'+8m'^2)+4F_4^2m'(3-4m'-2m'^2+4m'^3)))-2F_2^4J^2(32+16J^2(1+F_4^2+m'+m'^2)+J^{10}m'(1+m') (F_4^2+(-1+m')m')^2(F_4^4+(-1+m')^2m'^2-F_4^2m'(5+m'))+J^4(2+8m'+24m'^2-32m'^3+16m'^4-16F_4^2(3-7m' + 4m'^2))++J^8(2F_4^8+F_4^6(-1-8m'+8m'^2)+F_4^4(4m'-48m'^3)+2(-1+m')^2m'^3(1+2m'-2m'^2+m'^3)-4F_4^2m'^2 (5-15m'^2+9m'^3+4m'^4))+J^6(4F_4^6-16F_4^4m'-F_4^2(5+28m'-40m'^2+56m'^4)+m'(1+5m'-4m'^3-8m'^4+8m'^5)))) - F_2^2(64+16J^2(7+12m'+8m'^2)+4J^4(11-8F_4^4+24m'+160F_4^2m'+28m'^2-8m'^3+12m'^4)+J^{12}m'^2(1+m')^2 (F_4^2+(-1+m')m')^2(F_4^4+(-1+m')^2m'^2-2F_4^2m'(3+m'))+J^6(5+12m'+64m'^2+16m'^3+128F_4^2m'^3-72m'^4 - 32m'^5+64m'^6+32F_4^4(3+7m'+4m'^2))+J^{10}(F_4^8(5+12m'+8m'^2)+8F_4^6m'(-3-4m'+2m'^2+4m'^3)+8F_4^4m'^2 (5-15m'^2-9m'^3+4m'^4)-16F_4^2m'^3(3-7m'^2+6m'^4)+(-1+m')^2m'^4(7+6m'-9m'^2-4m'^3+8m'^4))+J^8(4F_4^8+ 32F_4^6(1+2m'+2m'^2)-8F_4^2m'(5-4m'^2+16m'^4)+2F_4^4(5-28m'-40m'^2+56m'^4)+m'^2(11+6m'-9m'^2-24m'^3 + 24m'^4-16m'^5+12m'^6))))$$

Again the above expression for spin conductance is independent of $'a'$ and sign of exchange interaction but dependent on magnitude of exchange interaction and the spin and magnetic moment of HSM.

1(b). The differential conductance in the zero bias $E = 0$ limit and in the tunneling $Z \to Large$ limit, vanishes:

$$G_C^0 = 0 \tag{9}$$

while the differential spin conductance in the zero bias $E = 0$ limit and in the tunneling $Z \to Large$ limit, is given by:

$$G_S^0 = \frac{A}{B}$$

Where

$$\begin{aligned}
A = & -((64J^2\sin^4(k_Fa)(-8F_2^2+8F_4^2-4F_2^2J^2+4F_4^2J^2+3F_2^4F_4^2J^4-3F_2^2F_4^4J^4+4F_2^2J^2m'+4F_4^2J^2m' \\
& +12F_2^2F_4^2J^4m'-4F_2^2J^2m'^2+4F_4^2J^2m'^2-3F_2^2J^4m'^2+3F_4^2J^4m'^2+6F_2^2J^4m'^3+6F_4^2J^4m'^3 \\
& -3F_2^2J^4m'^4+3F_4^2J^4m'^4-4J^2(F_2^4F_4^2J^2-F_2^2(1+F_4^4J^2-2m'-4F_4^2J^2m'+(2+J^2)m'^2-2J^2m'^3 \\
& +J^2m'^4)+F_4^2(1+2m'+(2+J^2)m'^2+2J^2m'^3+J^2m'^4))\cos(2k_Fa)+J^2(F_2^4F_4^2J^2+F_4^2m'(1+m')(4+J^2m'(1+m')) \\
& -F_2^2(F_4^4J^2-4F_4^2J^2m'+(-1+m')m'(4+J^2(-1+m')m')))\cos(4k_Fa)-8F_2^2J\sin(2k_Fa)+8F_4^2J\sin(2k_Fa) \\
& -4F_2^2J^3m'\sin(2k_Fa)-4F_4^2J^3m'\sin(2k_Fa)+4F_2^2J^3m'^2\sin(2k_Fa)-4F_4^2J^3m'^2\sin(2k_Fa) \\
& +2F_2^2J^3m'\sin(4k_Fa)+2F_4^2J^3m'\sin(4k_Fa)-2F_2^2J^3m'^2\sin(4k_Fa)+2F_4^2J^3m'^2\sin(4k_Fa))))
\end{aligned}$$

$$\begin{aligned}
B = & ((8+4J^2+4F_4^2J^2+3F_4^4J^4-4J^2m'-6F_4^2J^4m'+4J^2m'^2+3J^4m'^2+6F_4^2J^4m'^2-6J^4m'^3+3J^4m'^4 \\
& -4J^2(1+F_4^4J^2-2m'+(2+J^2)m'^2-2J^2m'^3+J^2m'^4+2F_4^2(1+J^2(-1+m')m'))\cos(2k_Fa) \\
& +J^2(F_4^2+(-1+m')m')(4+F_4^2J^2+J^2(-1+m')m')\cos(4k_Fa)+8J\sin(2k_Fa)-4F_4^2J^3\sin(2k_Fa) \\
& +4J^3m'\sin(2k_Fa)-4J^3m'^2\sin(2k_Fa)+2F_4^2J^3\sin(4k_Fa)-2J^3m'\sin(4k_Fa) \\
& +2J^3m'^2\sin(4k_Fa))(8+4J^2+4F_2^2J^2+3F_2^4J^4+4J^2m'+6F_2^2J^4m'+4J^2m'^2+3J^4m'^2 \\
& +6F_2^2J^4m'^2+6J^4m'^3+3J^4m'^4-4J^2(1+F_2^4J^2+2m'+(2+J^2)m'^2+2J^2m'^3+J^2m'^4 \\
& +2F_2^2(1+J^2m'(1+m')))\cos(2k_Fa)+J^2(F_2^2+m'+m'^2)(4+F_2^2J^2+J^2m'(1+m'))\cos(4k_Fa) \\
& +8J\sin(2k_Fa)-4F_2^2J^3\sin(2k_Fa)-4J^3m'\sin(2k_Fa)-4J^3m'^2\sin(2k_Fa) \\
& +2F_2^2J^3\sin(4k_Fa)+2J^3m'\sin(4k_Fa)+2J^3m'^2\sin(4k_Fa)))
\end{aligned}$$

This expression in contrast to the transparent regime $Z = 0$, depends on $'a'$ and sign of exchange interaction J in addition to spin and magnetic moment of HSM and magnitude of exchange interaction.

Thus, in the tunneling regime $Z \to Large$ and in absence of any voltage bias $E = 0$, we have pure spin conductance for our NMNIS junction in absence of any charge conductance. This is one of the main results of this work.

2. In the gap edge limit $E = \Delta$, the expression for differential charge conductance reduces to

$$G_C^0 = \frac{64+16J^2+64J^2m'^2}{16+8J^2+J^4+32J^2m'^2-8J^4m'^2+16J^4m'^4}, \tag{10}$$

this implies at the gap edge the charge conductance becomes independent of Z (transparency of contact) and spin of magnetic molecule S while it is dependent on magnitude of J, and magnetic moment m' of HSM. The spin conductance in this limit vanishes regardless of the values of J, S, m' and Z.

In the table below we tabulate the above results:

Differential Conductance ($\downarrow$)	Transparent case $Z = 0$	General case		
		$E = 0$		$E = \Delta$
		$Z = 0$	$Z = Large$	
G_C^0	$\frac{R_1}{Q_1} + \frac{R_2}{Q_2}$	$\frac{P}{Q}$	0	$\frac{64+16J^2+64J^2m'^2}{16+8J^2+J^4+32J^2m'^2-8J^4m'^2+16J^4m'^4}$
G_S^0	$\frac{P_1}{Q_1} - \frac{P_2}{Q_2}$	$\frac{R}{Q}$	$\frac{A}{B}$	0

III. CHARACTERIZING THE HIGH SPIN MOLECULE'S SPIN, MAGNETIC MOMENT AND INTERACTION STRENGTH

In Table I we tabulate the values of the differential spin and charge conductance for different values of spin (S) and magnetic moment (m') of the magnetic molecule in the zero bias limit, this limit implies the differential conductance is nothing but the total conductance. We further address the case for transparent contact ($Z = 0$) at the metal-superconductor interface. We see the differential charge conductance (G_C) is almost constant (however, there is a perceptible slight decrease in G_C for increasing m') for different magnetic moments m' for a particular value of S. The differential spin conductance on the other hand follows the relation $G_S\,|_{m'} = G_S\,|_{-m'}$ and can also be negative[17], further the magnitude of G_S increases with increasing magnitude of m' for a particular S. In Table II, we tabulate the charge and spin conductance again but for the energy at gap edge limit $E = \Delta$, here we see remarkably that the spin conductance is exactly zero while the charge conductance for a particular S varies with the value of magnetic moment but is independent of the sign. Further, for increasing magnitude of m', G_C decreases. So to characterize the ground state spin and magnetic moment of the high spin molecule we look at Table I and II in conjunction, we first determine spin of magnetic molecule S from G_C values of Table I then we determine magnitude of magnetic moment m' from G_C values of Table II, finally to determine the sign of magnetic moment we look at G_S values of Table I. We thus can characterize the total ground state spin and magnetic moment of the high spin molecule. In tables I and II we also feature the spin flip probabilities for magnetic impurity- F_2 when spin up electron is incident while F_4 is when spin down electron is incident.

In order to get a closed form empirical expression for the differential charge and spin conductance we first plot the differential charge conductance as function of the spin of magnetic molecule S for $E \to 0$, $E = 0.1\Delta$, $E = 0.5\Delta$, $E = \Delta$ limit for transparent ($Z = 0$) case in Fig. 6.

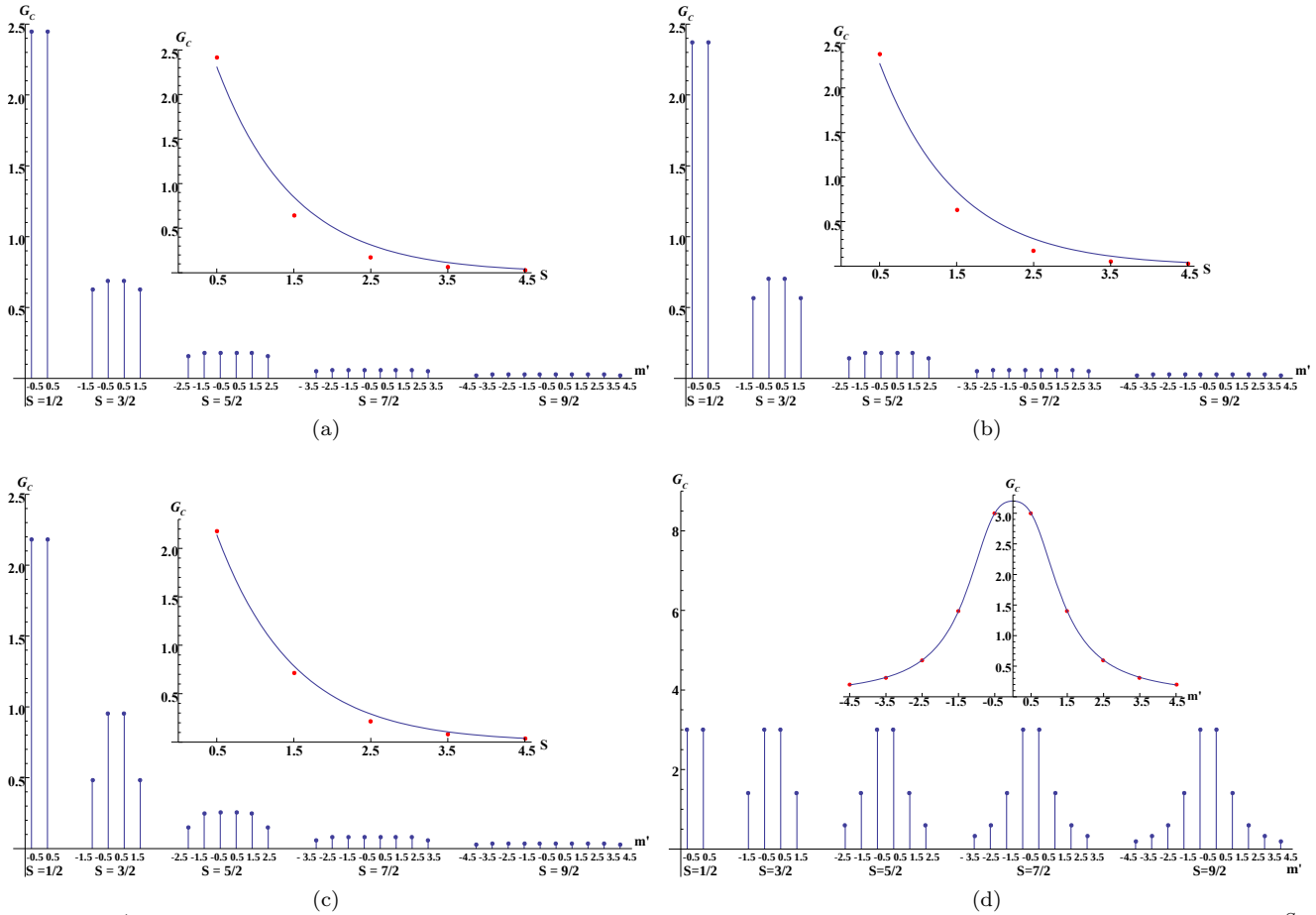

FIG. 6: a) *Charge conductance vs impurity spin plot for* $E = 0.001\Delta, J = 1, Z = 0$. *Here fitting function is* $3.87356e^{-S}$ *b)Charge conductance vs impurity spin plot for* $E = 0.1\Delta, J = 1, Z = 0$. *Here fitting function is* $3.75368e^{-S}$ *c) Charge conductance vs impurity spin plot for* $E = 0.5\Delta, J = 1, Z = 0$. *Here fitting function is* $3.53217e^{-S}$ *d) Charge conductance vs impurity spin plot for* $E = \Delta, J = 1$, *in d) the plot is independent of whether we are in transparent or tunneling regime.*

TABLE I: G_C and G_S values for different S and m' for $E = 0, J = 1, Z = 0$

S	m'	F_2	F_4	G_C	G_S
$\frac{1}{2}$	$-\frac{1}{2}$	1	0	2.44978	0.836601
	$\frac{1}{2}$	0	1	2.44978	-0.836601
$\frac{3}{2}$	$-\frac{3}{2}$	$\sqrt{3}$	0	0.62747	0.87213
	$-\frac{1}{2}$	2	$\sqrt{3}$	0.68701	-0.158463
	$\frac{1}{2}$	$\sqrt{3}$	2	0.68701	0.158463
	$\frac{3}{2}$	0	$\sqrt{3}$	0.62747	-0.87213
$\frac{5}{2}$	$-\frac{5}{2}$	$\sqrt{5}$	0	0.153586	0.486915
	$-\frac{3}{2}$	$2\sqrt{2}$	$\sqrt{5}$	0.178069	0.0344558
	$-\frac{1}{2}$	3	$2\sqrt{2}$	0.178689	-0.0106774
	$\frac{1}{2}$	$2\sqrt{2}$	3	0.178689	0.0106774
	$\frac{3}{2}$	$\sqrt{5}$	$2\sqrt{2}$	0.178069	-0.0344558
	$\frac{5}{2}$	0	$\sqrt{5}$	0.153586	-0.486915
$\frac{7}{2}$	$-\frac{7}{2}$	$\sqrt{7}$	0	0.0529872	0.241778
	$-\frac{5}{2}$	$2\sqrt{3}$	$\sqrt{7}$	0.0586056	0.0854991
	$-\frac{3}{2}$	$\sqrt{15}$	$2\sqrt{3}$	0.0602693	0.0269709
	$-\frac{1}{2}$	4	$\sqrt{15}$	0.0606785	0.00570319
	$\frac{1}{2}$	$\sqrt{15}$	4	0.0606785	-0.00570319
	$\frac{3}{2}$	$2\sqrt{3}$	$\sqrt{15}$	0.0602693	-0.0269709
	$\frac{5}{2}$	$\sqrt{7}$	$2\sqrt{3}$	0.0586056	-0.0854991
	$\frac{7}{2}$	0	$\sqrt{7}$	0.0529872	-0.241778
$\frac{9}{2}$	$-\frac{9}{2}$	3	0	0.0228349	0.129044
	$-\frac{7}{2}$	4	3	0.024257	0.0698984
	$-\frac{5}{2}$	$\sqrt{21}$	4	0.0249505	0.0367076
	$-\frac{3}{2}$	$2\sqrt{6}$	$\sqrt{21}$	0.0252736	0.017462
	$-\frac{1}{2}$	5	$2\sqrt{6}$	0.0253996	0.00512393
	$\frac{1}{2}$	$2\sqrt{6}$	5	0.0253996	-0.00512393
	$\frac{3}{2}$	$\sqrt{21}$	$2\sqrt{6}$	0.0252736	-0.017462
	$\frac{5}{2}$	4	$\sqrt{21}$	0.0249505	-0.0367076
	$\frac{7}{2}$	3	4	0.024257	-0.0698984
	$\frac{9}{2}$	0	3	0.0228349	-0.129044

A. Characterizing the spin S of HSM

A least square fit in Figs. 6(a-c) indicates that the charge conductance exponentially decays with the spin (S) of the magnetic molecule, thus $G_C \propto exp(-S)$. To plot the Figs. 6(a-c) we take the mean charge conductance for a particular S the reason being although G_C is fairly constant for different values of m' there is a slight decrease for increasing magnitude of m'. One can also see the charge conductance does not change dramatically from the zero

TABLE II: G_C and G_S values for different S and m' for $E = \Delta$, $J = 1$, $Z = 0$

S	m'	F_2	F_4	G_C	G_S
$\frac{1}{2}$	$-\frac{1}{2}$	1	0	3	0
	$\frac{1}{2}$	0	1	3	0
$\frac{3}{2}$	$-\frac{3}{2}$	$\sqrt{3}$	0	1.4	0
	$-\frac{1}{2}$	2	$\sqrt{3}$	3	0
	$\frac{1}{2}$	$\sqrt{3}$	2	3	0
	$\frac{3}{2}$	0	$\sqrt{3}$	1.4	0
$\frac{5}{2}$	$-\frac{5}{2}$	$\sqrt{5}$	0	0.6	0
	$-\frac{3}{2}$	$2\sqrt{2}$	$\sqrt{5}$	1.4	0
	$-\frac{1}{2}$	3	$2\sqrt{2}$	3	0
	$\frac{1}{2}$	$2\sqrt{2}$	3	3	0
	$\frac{3}{2}$	$\sqrt{5}$	$2\sqrt{2}$	1.4	0
	$\frac{5}{2}$	0	$\sqrt{5}$	0.6	0
$\frac{7}{2}$	$-\frac{7}{2}$	$\sqrt{7}$	0	0.317647	0
	$-\frac{5}{2}$	$2\sqrt{3}$	$\sqrt{7}$	0.6	0
	$-\frac{3}{2}$	$\sqrt{15}$	$2\sqrt{3}$	1.4	0
	$-\frac{1}{2}$	4	$\sqrt{15}$	3	0
	$\frac{1}{2}$	$\sqrt{15}$	4	3	0
	$\frac{3}{2}$	$2\sqrt{3}$	$\sqrt{15}$	1.4	0
	$\frac{5}{2}$	$\sqrt{7}$	$2\sqrt{3}$	0.6	0
	$\frac{7}{2}$	0	$\sqrt{7}$	0.317647	0
$\frac{9}{2}$	$-\frac{9}{2}$	3	0	0.19457	0
	$-\frac{7}{2}$	4	3	0.317647	0
	$-\frac{5}{2}$	$\sqrt{21}$	4	0.6	0
	$-\frac{3}{2}$	$2\sqrt{6}$	$\sqrt{21}$	1.4	0
	$-\frac{1}{2}$	5	$2\sqrt{6}$	3	0
	$\frac{1}{2}$	$2\sqrt{6}$	5	3	0
	$\frac{3}{2}$	$\sqrt{21}$	$2\sqrt{6}$	1.4	0
	$\frac{5}{2}$	4	$\sqrt{21}$	0.6	0
	$\frac{7}{2}$	3	4	0.317647	0
	$\frac{9}{2}$	0	3	0.19457	0

energy limit as is evident from Fig. 6(b), $E = 0.1\Delta$ and 6(c) $E = 0.5\Delta$. This approximate relation $G_C \propto exp(-S)$ for the charge conductance implies that one can exactly characterize the spin (S) of the magnetic molecule irrespective of the voltage applied at the metal superconductor interface as long as we are below the gap. The situation changes at and near the gap edge $E = \Delta$, shown in Fig. 6(d), herein the charge conductance does not vary with S, and the variation with m' for different S is also uniform.

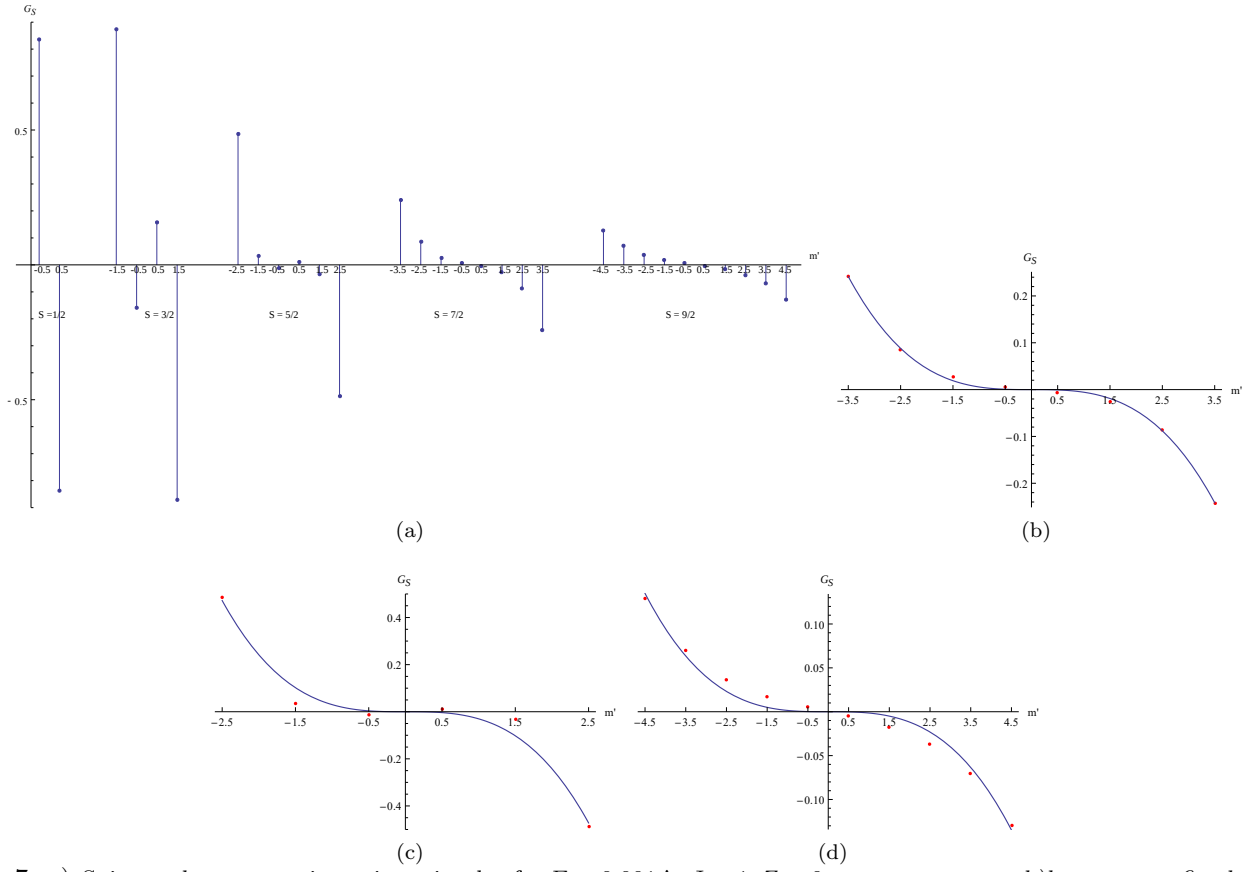

FIG. 7: a) *Spin conductance vs impurity spin plot for* $E = 0.001\Delta, J = 1, Z = 0$ *transparent case, b)least square fit plot for* $S = 7/2, E = 0.001\Delta, J = 1, Z = 0$. *Here fitting function is* $-0.00563217m'^3$ *c)least square fit plot for* $S = 5/2, E = 0.001\Delta, J = 1, Z = 0$. *Here fitting function is* $-0.030217m'^3$ *d)least square fit plot for* $S = 9/2, E = 0.001\Delta, J = 1, Z = 0$. *Here fitting function is* $-0.00147997m'^3$

B. Characterizing the magnetic moment m' of HSM

Next we plot the spin conductance again for transparent case ($Z = 0$) in Fig. 7 and for the tunneling regime in Fig. 8. Unlike the charge conductance the spin conductance does not show any definite pattern as function of S, apart from the fact that as S increases there is a monotonic decrease in spin conductance. However, an interesting pattern emerges when the spin conductance is plotted for a particular S as function of the magnetic moment m', in this case as one can make out that a least square fit for transparent case($Z = 0$) takes the general form $G_S \propto -m'^3$, but for the tunneling regime it takes the general form $G_S \propto -m'$.

C. Characterizing the magnitude and nature of exchange interaction between HSM and electron/hole in system

In Fig. 9 we have plotted charge conductance as a function of J for a high spin molecule (S=5/2). We see that as the magnetic moment (m') increases charge conductance decreases. The variation of G_C with J is Gaussian. The least square function fits are plotted too, these are for plot Fig 9(b) ($E = 0, Z = 0, S = 5/2$) the fit function is $G_C = 0.205391/(1+1.89909J^2)+3.85544*Exp(-4.35542J^2)$, in the E=0 limit the charge conductance is independent of magnetic moment m'. For Fig. 9(a) ($E = \Delta, Z = 0, S = 5/2$) for $m' = 5/2$ fit function is $G_C = 3.71424/(1 + 5.19513J^2) + 0.284056 * Exp(-21.4233J^2)$ for $m' = 3/2$ fit function $G_C = 3.63184/(1 + 2.36191J^2) + 0.35078 * Exp(-0.160939J^2)$ for $m' = 1/2$ fit function $G_C = 2+2/(1+J^2)$. This helps in estimating the strength of interaction, however the sign of interaction remains undecipherable from this plot. To estimate the sign of interaction we plot the derivative of differential spin conductance (dG_S/dJ) with respect to J in Fig. 9(c). We can clearly see that this quantity is anti-symmetric with respect to J, enabling us to detect the nature of interaction of electrons/holes in the system with the HSM.

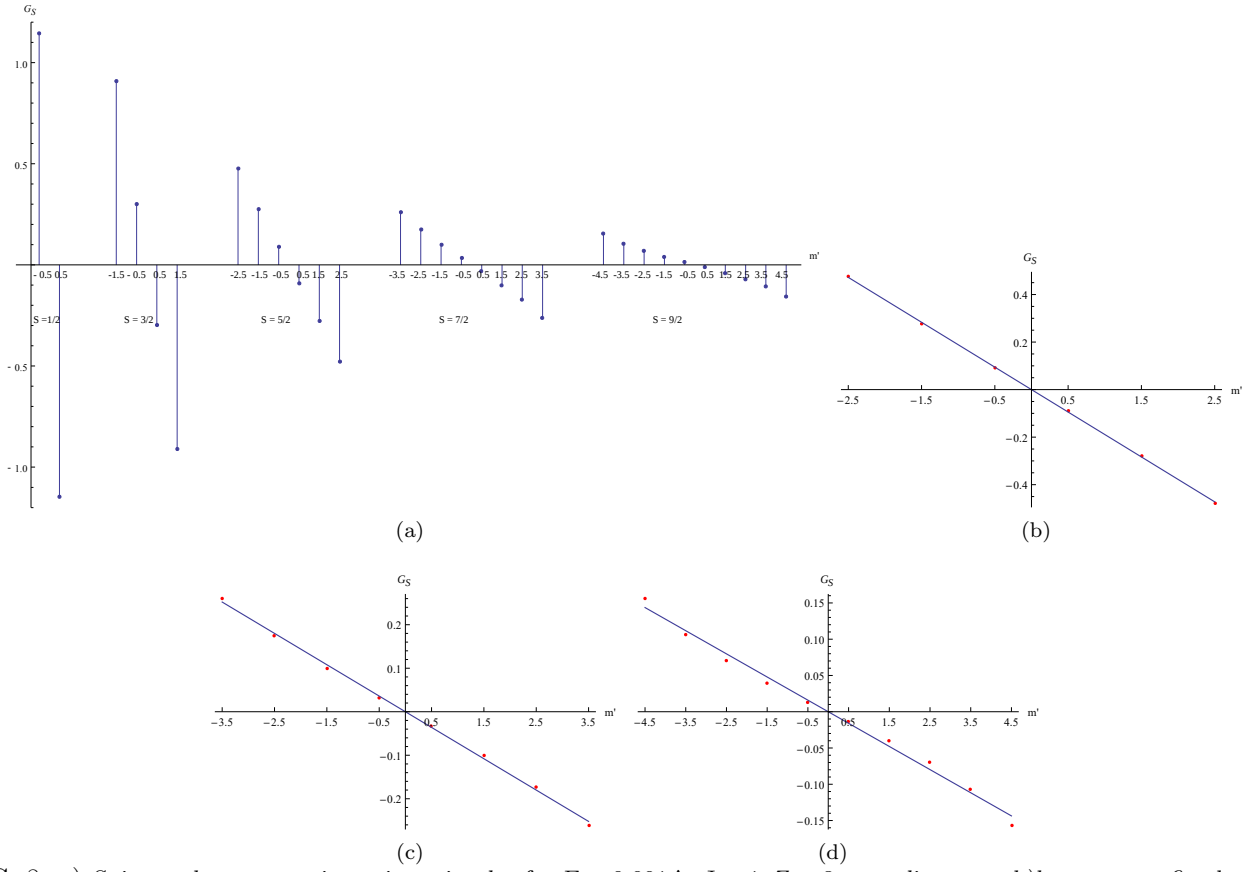

FIG. 8: a) *Spin conductance vs impurity spin plot for* $E = 0.001\Delta, J = 1, Z = 3$ *tunneling case, b)least square fit plot for* $S = 5/2, E = 0.001\Delta, J = 1, Z = 3$. *Here fitting function is* $-0.160742m'$ *c)least square fit plot for* $S = 7/2, E = 0.001\Delta, J = 1, Z = 3$. *Here fitting function is* $-0.0555307m'$ *d)least square fit plot for* $S = 9/2, E = 0.001\Delta, J = 1, Z = 3$. *Here fitting function is* $-0.0237177m'$

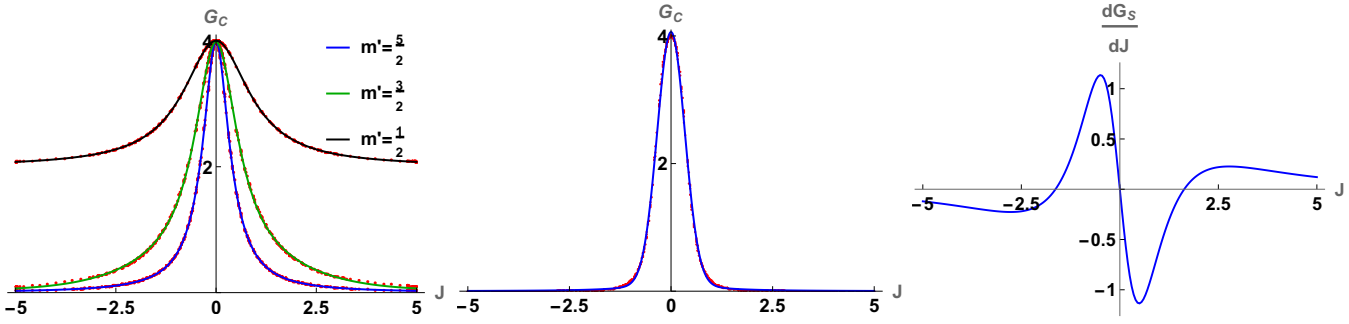

FIG. 9: Charge conductance vs. exchange interaction strength J for(a) $S = 5/2$ and different values of magnetic moment of molecule. Other parameters are $Z = 0$, and $E = \Delta$. (b) S=5/2 $E = 0, Z = 0$. For this case conductance becomes independent of m' and (c) The derivative of differential spin conductance with respect to J. Regardless of S, m', $\frac{dGs}{dJ}$ is antisymmetric with respect to the nature of interaction. From this plot we can note the sign of the interaction.

IV. APPLICATION TO SPINTRONICS: PURE SPIN CONDUCTANCE IN ABSENCE OF CHARGE

Next in Fig. 10 we compare the differential spin and charge conductance for NIS, FIS and NMNIS junctions in the transparent limit(Z=0). Further, the polarization in Ferromagnet is 90% (as is indicated in (a) $h_0 = 0.9E_F$). The parameters for NMNIS are mentioned in Figure itself. In Fig. 10(a) the differential spin conductance is plotted, it shows remarkably that there is a finite spin conductance below the gap in case of a NMNIS junction in contrast to

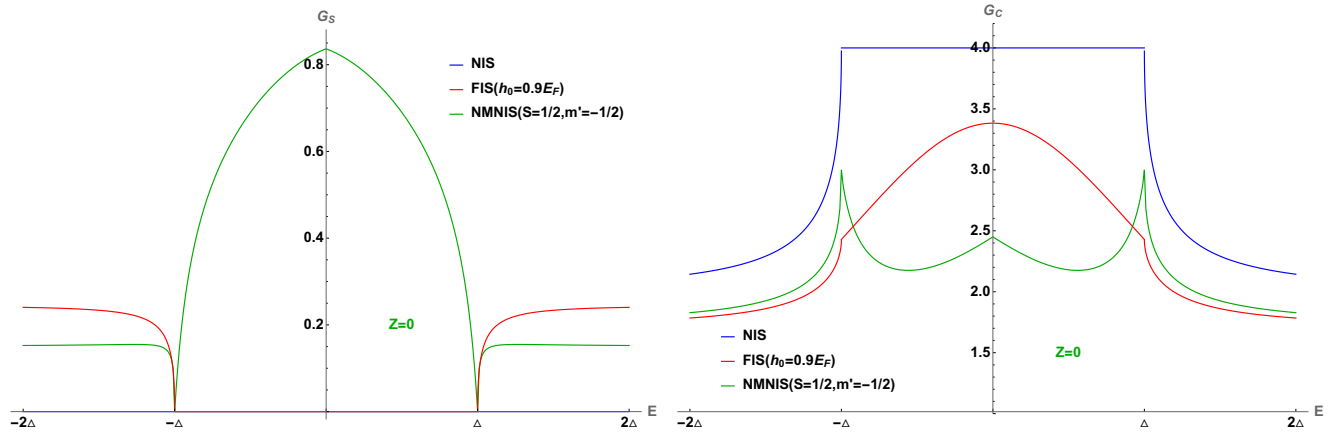

(a) (b)

FIG. 10: a) *Spin conductance and (b) Charge conductance for NIS, FIS and NMNIS junctions in the transparent regime. Note the absence of any spin conductance below the gap for NIS and FIS junction.*

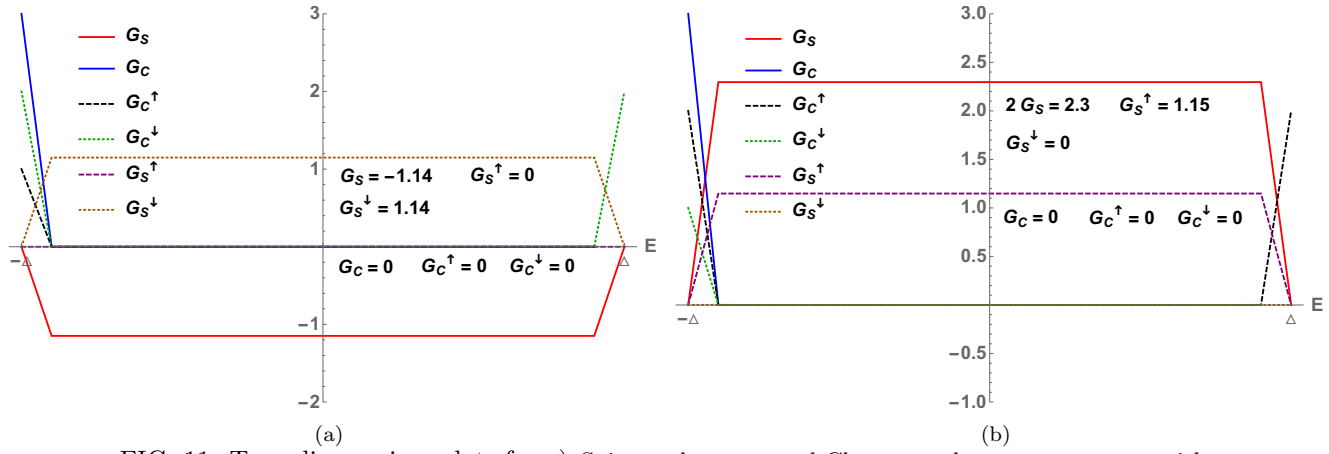

(a) (b)

FIG. 11: Tunneling regime plots for a) *Spin conductance and Charge conductance vs energy with* $J = 1, Z = 10, S = 1/2, m' = 1/2$ *b) Spin conductance and Charge conductance vs energy with* $J = 1, Z = 10, S = 1/2, m' = -1/2$. *Note the exclusive pure spin conductance (only spin down electrons contribute) in absence of any charge for (a) and exclusive pure spin conductance (only spin up electrons contribute) in absence of any charge for (b).*

either a FIS or NIS junction. In Fig. 10(b), we plot the charge conductance (G_C), while in the NIS junction G_C is quantized at 4. On the other hand for a FIS junction, it is always less than 4 and beyond a peak at $E = 0$, G_C continuously decreases. In the NMNIS junction, however there is a peak not only at $E = 0$, there are peaks also at $E = \pm\Delta$. Further, in Fig. 11 (a) and (b) we plot G_C and G_S along-with the individual up-spin($G_S^{\uparrow}$) and down-spin($G_S^{\downarrow}$) conductances. We see in Fig. 11(b) that pure spin conductance with only selective transport of spin-up without any charge transport while in Fig. 11(a) it is shown that pure spin conductance with only selective transport of spin-down without any charge transport. Finally, in Fig. 12(a) and (b) the charge and spin conductances are plotted for HSM with $S = 1/2$ and $m' = \pm 1/2$ as function of the transparency of the junction Z. The charge conductance is independent of the sign spin magnetic moment m' but the spin conductance is dependent and it has to be noted that the spin conductance has same magnitude but opposite sign for different sign of m'. To check what happens when we increase S we plot G_C and G_S as function of Z in Fig. 12(c) and (d) for $S = 5/2$ and different values of possible spin magnetic moment $m' = -5/2, -3/2, -1/2, 1/2, 3/2, 5/2$. G_C being independent of sign of m' but depends on the magnitude of m'. One thing which is quite apparent is that as Z increases into the tunneling regime greater than 3, $G_C \to 0$. G_S on the other hand in the tunneling regime is constant and finite and the magnitude of spin conductance increases with the magnitude of spin magnetic moment.

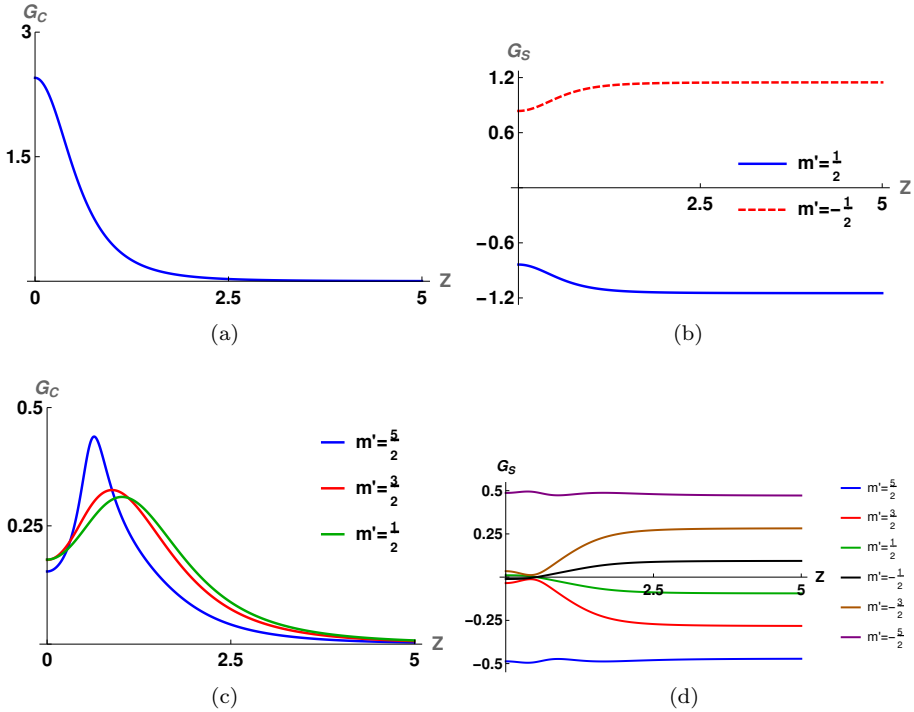

FIG. 12: a) *Charge conductance vs Z plot for* $J = 1, S = 1/2, E = 0$ *b)Spin conductance vs Z plot for* $J = 1, S = 1/2, E = 0$ *c)Charge conductance vs Z plot for* $J = 1, S = 5/2, E = 0$ *d)Spin conductance vs Z plot for* $J = 1, S = 5/2, E = 0$.

V. CONCLUSIONS AND EXPERIMENTAL REALIZATION

To conclude, we aimed to fulfill two objectives with our set-up as outlined in the Introduction. The first of fully characterizing a HSM was accomplished using the charge and spin conductance of the NMNIS junction at the zero bias limit $E = 0$ and the gap edge limit $E = \Delta$. The second aim of pure spin conductance without any accompanying charge conductance was realized in the tunneling *Zlarge* limit. The set-up as envisaged in Fig. 1(a) and (b), can be easily realized in the lab. The NIS junctions have been experimentally realized since more than 30 years. High spin Molecules have been realized since 20 years. The amalgamation of a NIS junction with a HSM shouldn't be difficult. Especially with a s-wave superconductor like Aluminium or Niobium it should be perfectly possible. In future junctions with HSM and High T_c superconductors will be attempted, this will have the additional aspect of nodes in the superconducting gap, and the aim would be to exploit it for spintronics.

ACKNOWLEDGMENTS

This work was supported by the grant "Non-local correlations in nanoscale systems: Role of decoherence, interactions, disorder and pairing symmetry" from SCIENCE & ENGINEERING RESEARCH BOARD, New Delhi, Government of India, Grant No. EMR/2015/001836, Principal Investigator: Dr. Colin Benjamin, National Institute of Science Education and Research, Bhubaneswar, India.

VI. APPENDIX: IMPOSING BOUNDARY CONDITIONS IN THE METAL-MAGNETIC MOLECULE-SUPERCONDUCTOR JUNCTION

A. Boundary conditions

At $x = 0$

$$\psi_N^I(x) = \psi_N^{II}(x), \text{(continuity of wavefunctions)} \tag{11}$$

$$\frac{d\psi_N^{II}}{dx} - \frac{d\psi_N^{I}}{dx} = -\frac{2m^\star J_0 \vec{s}.\vec{S}}{\hbar^2}\psi_N^I, \text{(discontinuity in first derivative)} \tag{12}$$

At $x = a$

$$\psi_N^{II}(x) = \psi_S(x), \text{(continuity of wavefunctions)} \tag{13}$$

$$\frac{d\psi_S}{dx} - \frac{d\psi_N^{II}}{dx} = \frac{2m^\star V}{\hbar^2}\psi_N^{II}, \text{(discontinuity in first derivative)} \tag{14}$$

From boundary conditions (3) and (5) we get

$$1 + r_e^{\uparrow\uparrow} = t_e^{'\uparrow\uparrow} + b_e^{\uparrow\uparrow}e^{ik_e a}$$

$$r_e^{\uparrow\downarrow} = t_e^{'\uparrow\downarrow} + b_e^{\uparrow\downarrow}e^{ik_e a}$$

$$r_h^{\uparrow\uparrow} = c_h^{\uparrow\uparrow}e^{-ik_h a} + a_h^{\uparrow\uparrow}$$

$$r_h^{\uparrow\downarrow} = c_h^{\uparrow\downarrow}e^{-ik_h a} + a_h^{\uparrow\downarrow}$$

$$t_e^{'\uparrow\uparrow}e^{ik_e a} + b_e^{\uparrow\uparrow} = t_e^{\uparrow\uparrow}ue^{iq_+ a} + t_h^{\uparrow\downarrow}ve^{-iq_- a}$$

$$t_e^{'\uparrow\downarrow}e^{ik_e a} + b_e^{\uparrow\downarrow} = t_e^{\uparrow\downarrow}ue^{iq_+ a} + t_h^{\uparrow\uparrow}ve^{-iq_- a}$$

$$c_h^{\uparrow\uparrow} + a_h^{\uparrow\uparrow}e^{-ik_h a} = t_h^{\uparrow\uparrow}ue^{-iq_- a} + t_e^{\uparrow\downarrow}ve^{iq_+ a}$$

$$c_h^{\uparrow\downarrow} + a_h^{\uparrow\downarrow}e^{-ik_h a} = t_h^{\uparrow\downarrow}ue^{-iq_- a} + t_e^{\uparrow\uparrow}ve^{iq_+ a}$$

From Ref. 13, we have-

$$\vec{s}.\vec{S} = s^Z S^Z + \frac{1}{2}(s^- S^+ + s^+ S^-) \tag{15}$$

Here $s^\pm = s_x \pm i s_y$ and $S^\pm = S_x \pm i S_y$ are the raising and lowering spin operators.
For spin up electron component

$$\vec{s}.\vec{S}\begin{bmatrix}1\\0\\0\\0\end{bmatrix}\phi_{m'}^S = mm'\begin{bmatrix}1\\0\\0\\0\end{bmatrix}\phi_{m'}^S + \frac{1}{2}F_1F_2\begin{bmatrix}0\\1\\0\\0\end{bmatrix}\phi_{m'+1}^S$$

Foe spin down electron component

$$\vec{s}.\vec{S}\begin{bmatrix}0\\1\\0\\0\end{bmatrix}\phi_{m'+1}^S = (m-1)(m'+1)\begin{bmatrix}0\\1\\0\\0\end{bmatrix}\phi_{m'+1}^S + \frac{1}{2}F_1F_2\begin{bmatrix}1\\0\\0\\0\end{bmatrix}\phi_{m'}^S$$

For spin up hole component

$$\vec{s}.\vec{S}\begin{bmatrix}0\\0\\1\\0\end{bmatrix}\phi_{m'}^S = mm'\begin{bmatrix}0\\0\\1\\0\end{bmatrix}\phi_{m'}^S + \frac{1}{2}F_1F_2\begin{bmatrix}0\\0\\0\\1\end{bmatrix}\phi_{m'+1}^S$$

For spin down hole component

$$\vec{s}.\vec{S}\begin{bmatrix}0\\0\\0\\1\end{bmatrix}\phi^S_{m'+1}=(m-1)(m'+1)\begin{bmatrix}0\\0\\0\\1\end{bmatrix}\phi^S_{m'+1}+\frac{1}{2}F_1F_2\begin{bmatrix}0\\0\\1\\0\end{bmatrix}\phi^S_{m'}$$

where m and m' are the electron spin and impurity spin respectively. $F_1=\sqrt{(s+m)(s-m+1)}$ and $F_2=\sqrt{(S-m')(S+m'+1)}$. Now from boundary condition (4) after some algebraic manipulation we get

$$ik_e[t_e^{'\uparrow\uparrow}-b_e^{\uparrow\uparrow}e^{ik_ea}-1+r_e^{\uparrow\uparrow}]=-(m^\star J_0/\hbar^2)[2mm'(1+r_e^{\uparrow\uparrow})+F_1F_2r_e^{\uparrow\downarrow}]$$

$$ik_e[t_e^{'\uparrow\downarrow}-b_e^{\uparrow\downarrow}e^{ik_ea}+r_e^{\uparrow\downarrow}]=-(m^\star J_0/\hbar^2)[2(m-1)(m'+1)r_e^{\uparrow\downarrow}+F_1F_2(1+r_e^{\uparrow\uparrow})]$$

$$ik_h[c_h^{\uparrow\uparrow}e^{-ik_ha}-a_h^{\uparrow\uparrow}-r_h^{\uparrow\uparrow}]=-(m^\star J_0/\hbar^2)[2mm'r_h^{\uparrow\uparrow}+F_1F_2r_h^{\uparrow\downarrow}]$$

$$ik_h[c_h^{\uparrow\downarrow}e^{-ik_ha}-a_h^{\uparrow\downarrow}-r_h^{\uparrow\downarrow}]=-(m^\star J_0/\hbar^2)[2(m-1)(m'+1)r_h^{\uparrow\downarrow}+F_1F_2r_h^{\uparrow\uparrow}]$$

From boundary condition (6) after some algebraic calculation we get

$$iq_+t_e^{\uparrow\uparrow}ue^{iq_+a}-iq_-t_h^{\uparrow\downarrow}ve^{-iq_-a}-ik_et_e^{'\uparrow\uparrow}e^{ik_ea}+ik_eb_e^{\uparrow\uparrow}=(2m^\star V/\hbar^2)[t_e^{'\uparrow\uparrow}e^{ik_ea}+b_e^{\uparrow\uparrow}]$$

$$iq_+t_e^{\uparrow\downarrow}ue^{iq_+a}-iq_-t_h^{\uparrow\uparrow}ve^{-iq_-a}-ik_et_e^{'\uparrow\downarrow}e^{ik_ea}+ik_eb_e^{\uparrow\downarrow}=(2m^\star V/\hbar^2)[t_e^{'\uparrow\downarrow}e^{ik_ea}+b_e^{\uparrow\downarrow}]$$

$$iq_+t_e^{\uparrow\downarrow}ve^{iq_+a}-iq_-t_h^{\uparrow\uparrow}ue^{-iq_-a}-ik_hc_h^{\uparrow\uparrow}+ik_ha_h^{\uparrow\uparrow}e^{-ik_ha}=(2m^\star V/\hbar^2)[c_h^{\uparrow\uparrow}+a_h^{\uparrow\uparrow}e^{-ik_ha}]$$

$$iq_+t_e^{\uparrow\uparrow}ve^{iq_+a}-iq_-t_h^{\uparrow\downarrow}ue^{-iq_-a}-ik_hc_h^{\uparrow\downarrow}+ik_ha_h^{\uparrow\downarrow}e^{-ik_ha}=(2m^\star V/\hbar^2)[c_h^{\uparrow\downarrow}+a_h^{\uparrow\downarrow}e^{-ik_ha}]$$

In Andreev approximation we take $k_e=k_h=q_+=q_-=k_F$. So finally we get

$$\begin{aligned}
r_e^{\uparrow\uparrow}-t_e^{'\uparrow\uparrow}-b_e^{\uparrow\uparrow}e^{ik_Fa}&=-1\\
r_e^{\uparrow\downarrow}-t_e^{'\uparrow\downarrow}-b_e^{\uparrow\downarrow}e^{ik_Fa}&=0\\
r_h^{\uparrow\uparrow}-c_h^{\uparrow\uparrow}e^{-ik_Fa}-a_h^{\uparrow\uparrow}&=0\\
r_h^{\uparrow\downarrow}-c_h^{\uparrow\downarrow}e^{-ik_Fa}-a_h^{\uparrow\downarrow}&=0\\
t_e^{'\uparrow\uparrow}e^{ik_Fa}+b_e^{\uparrow\uparrow}-t_e^{\uparrow\uparrow}ue^{ik_Fa}-t_h^{\uparrow\downarrow}ve^{-ik_Fa}&=0\\
t_e^{'\uparrow\downarrow}e^{ik_Fa}+b_e^{\uparrow\downarrow}-t_h^{\uparrow\uparrow}ve^{-ik_Fa}-t_e^{\uparrow\downarrow}ue^{ik_Fa}&=0\\
c_h^{\uparrow\uparrow}+a_h^{\uparrow\uparrow}e^{-ik_Fa}-t_h^{\uparrow\uparrow}ue^{-ik_Fa}-t_e^{\uparrow\downarrow}ve^{ik_Fa}&=0\\
c_h^{\uparrow\downarrow}+a_h^{\uparrow\downarrow}e^{-ik_Fa}-t_e^{\uparrow\uparrow}ve^{ik_Fa}-t_h^{\uparrow\downarrow}ue^{-ik_Fa}&=0\\
(1-i2Jmm')r_e^{\uparrow\uparrow}-iJF_1F_2r_e^{\uparrow\downarrow}+t_e^{'\uparrow\uparrow}-b_e^{\uparrow\uparrow}e^{ik_Fa}&=(1+i2Jmm')\\
iJF_1F_2r_e^{\uparrow\uparrow}+(i2J(m-1)(m'+1)-1)r_e^{\uparrow\downarrow}-t_e^{'\uparrow\downarrow}+b_e^{\uparrow\downarrow}e^{ik_Fa}&=-iJF_1F_2\\
(1+i2Jmm')r_h^{\uparrow\uparrow}+iJF_1F_2r_h^{\uparrow\downarrow}-e^{-ik_Fa}c_h^{\uparrow\uparrow}+a_h^{\uparrow\uparrow}&=0\\
iJF_1F_2r_h^{\uparrow\uparrow}+(1+i2J(m-1)(m'+1))r_h^{\uparrow\downarrow}-c_h^{\uparrow\downarrow}e^{-ik_Fa}+a_h^{\uparrow\downarrow}&=0\\
(i2Z-1)e^{ik_Fa}t_e^{'\uparrow\uparrow}+(1+i2Z)b_e^{\uparrow\uparrow}+t_e^{\uparrow\uparrow}ue^{ik_Fa}-t_h^{\uparrow\downarrow}ve^{-ik_Fa}&=0\\
(i2Z-1)e^{ik_Fa}t_e^{'\uparrow\downarrow}+(1+i2Z)b_e^{\uparrow\downarrow}+t_e^{\uparrow\downarrow}ue^{ik_Fa}-t_h^{\uparrow\uparrow}ve^{-ik_Fa}&=0\\
(i2Z-1)c_h^{\uparrow\uparrow}+(i2Z+1)e^{-ik_Fa}a_h^{\uparrow\uparrow}-t_h^{\uparrow\uparrow}ue^{-ik_Fa}+t_e^{\uparrow\downarrow}ve^{ik_Fa}&=0\\
(i2Z-1)c_h^{\uparrow\downarrow}+(i2Z+1)e^{-ik_Fa}a_h^{\uparrow\downarrow}-t_h^{\uparrow\downarrow}ue^{-ik_Fa}+t_e^{\uparrow\uparrow}ve^{ik_Fa}&=0
\end{aligned}$$

where $J = \frac{m^\star J_0}{\hbar^2 k_F}$ and $Z = \frac{m^\star V}{\hbar^2 k_F}$.

---

* colin.nano@gmail.com

[1] R. J. Soulen, et. al., Science 282, 8588 (1998).
[2] C. Tsuei and J. Kirtley, Rev. Mod. Phys. 72, 970 (2000).
[3] Colin Benjamin, Phys. Rev. B 71, 174512 (2005); Colin Benjamin, Phys. Rev. B (Rapid Communication) 74, 180503(R) (2006).
[4] A. Schweiger, G. Jeschke "Principles of pulse electron paramagnetic resonance", Oxford University Press, 2001; T. Takui in "Molecular Magnetism" K.Itoh, M. Kinoshita (eds) Kodansha and Gordon and Breach, Tokyo 2000.
[5] H. Kurreck, B. Kirste, W. Lubitz (eds.) "Electron Nuclear Double Resonance Spectroscopy of Radicals in Solutions", Chapter 8, Weinheim 1988
[6] Y. Rechkemmer, et. al., Nature Comms. 7: 10467 (2016).
[7] Matthias Eschrig, Physics Today 64(1), 43(2011)
[8] Firoz Islam and Colin Benjamin, J. Phys.: Condens. Matter 28 (2016) 035305.
[9] M. Misiorny and J. Barnas, Phys. Rev. B 76, 054448 (2007); Phys Rev B 75, 134425 (2007)
[10] Henrik Enoksen , Jacob Linder and Asle Sudbo, Phys Rev B 85,014512 (2012).
[11] G. E. Blonder, M.Tinkham, and T.M.Klapwijk, Phys Rev B 25, 4515 (1982).
[12] D. Aravena, D. Venegas-Yazigi & E. Ruiz, Scientific Reports 6, Article number: 23847 (2016).
[13] O. L. T. de Menezes and J. S. Helman, American Journal of Physics 53, 1100 (1985).
[14] M. J. M. de Jong and C. W. J. Beenakker, Phys. Rev. Lett. 74, 1657 (1995).
[15] Q. Cheng and B. Jin, Physica B 426, 42 (2013).
[16] S. Kashiwaya, et. al., Phys. Rev. B 60, 352 (1999); Y. Tanaka, et. al., Phys. Rev. B 79, 060505 (2009).
[17] Y. Tanaka, et. al., Phys. Rev. B 79, 060505 (2009).